

Magnetic levitation force and penetration depth in type-II superconductors

J. H. Xu, J. H. Miller, Jr., and C. S. Ting

Department of Physics and Texas Center for Superconductivity, University of Houston, Houston, Texas 77204

(Received 21 July 1994)

The superconducting levitation force F acting on a magnet placed above a type-II superconductor in both Meissner and mixed states is calculated as a function of temperature, based upon the London model. A simple relationship between the levitation force and the London penetration depth λ is found. In particular, in the limit of $a/\lambda \gg 1$, where a is the separation between the magnet and the superconductor, F varies linearly with λ , regardless of the shape of the magnet. The temperature dependences of λ and F are examined for various superconducting pairing states, including s -wave, d -wave, and $s + id$ states. It is found that, at low temperatures, both λ and F show an exponential temperature dependence for s -wave, linear- T for d -wave, and T^2 dependence in a wide low-temperature range for the $s + id$ state with a dominant d -wave component. The magnetic force microscope (MFM) is proposed to accurately measure the temperature-dependent levitation force. It is shown that the microscopic size of the MFM tip enables one to obtain the intrinsic temperature-dependent penetration depth of a single grain, in spite of the overall quality of the superconducting sample.

I. INTRODUCTION

The temperature dependence of the London penetration depth $\lambda(T)$ is often used as a means of distinguishing between different models in superconductivity because at low temperatures $\lambda(T)$ reflects changes in the superfluid density responsible for screening of electromagnetic fields. In s -wave BCS theory, this quantity has an exponential temperature dependence due to the presence of an energy gap.¹ A number of other possible pairing states, involving more complicated gap functions, have been suggested for heavy-fermion and high-temperature superconductors.²⁻⁵ For example, the d -wave pairing state has low-energy excitations that can result in a temperature dependence of $\lambda(T)$ which differs from the exponentially activated behavior of conventional BCS superconductors. Thus, accurate determination of the temperature dependence of $\lambda(T)$ is of crucial importance in the study of superconductivity, because it can provide information about the symmetry of the pairing state. Recently, there have been numerous measurements of the London penetration depth in heavy-fermion^{6,7} and high-temperature superconductors.⁸⁻¹¹ The most common methods used thus far to measure $\lambda(T)$ are complicated microwave techniques.

We emphasize that the value of λ determined *macroscopically*, from microwave techniques,⁸⁻¹¹ represents the intrinsic London penetration depth only for a perfect single crystal. However, if the superconductor is not a perfect single crystal, then, these *macroscopic* measurements only provide an effective averaged magnetic penetration depth. In particular, the short coherence length of high- T_c superconductors (HTS) makes these materials unusually sensitive to structural imperfections, such as grain boundaries. Even so-called HTS single crystals or high-quality thin films usually contain twin boundaries. The presence of grain boundaries, screw dislocations, and other imperfections in HTS materials lead to difficulties in

directly observing their fundamental physical properties. Most standard experimental techniques only access averaged information, from which the fundamental properties have to be derived with the use of theoretical models. Indeed, experimental data on the penetration depth based on *macroscopic* measurements at low temperatures depend dramatically on the sample quality. Klein *et al.*¹¹ reported a weak exponential temperature dependence, whereas Ma *et al.* found good agreement with T^2 variation, except for small deviations below 10 K.¹⁰ In contradiction with these results, a linear temperature dependence was reported by Hardy *et al.*⁹ and interpreted by the authors as an indication of d -wave superconductivity. All these measurements were reported to be performed on "high quality thin films or single crystals," but, nevertheless, yielded significantly different results. This shows that *macroscopic* measurements of λ are sample dependent and do not give the *intrinsic* temperature dependence of the London penetration depth, as argued by many authors.¹²⁻¹⁵ Clearly, it is important to clarify the *intrinsic* temperature dependence of the penetration depth, or of related physical quantities, in high- T_c superconductors.

In this work, we present an alternative method of determining the penetration depth. The approach is based on measurements of the superconducting levitation force acting on a magnet.¹⁶⁻¹⁸ We show that, at low temperatures, there exists a simple relationship between the levitation force and the London penetration depth. In particular, when $a/\lambda \gg 1$, where a is the separation between the magnet and the superconductor, the levitation force varies *linearly* with λ , regardless of the shape of the magnet. This result provides a new method of measuring the penetration depth, namely, one can determine λ directly from the measurements of the superconducting levitation force.

We propose that the temperature-dependent levitation force can accurately be measured using the magnetic

force microscope (MFM). We know that MFM (Refs. 19 and 20) is a method that was originally developed as an extension of atomic force microscopy (AFM).²¹ An MFM consists of a tiny magnetic tip which, when placed close to a magnetic sample, interacts with the stray magnetic field from the sample. The force exerted on the scanned tip is measured as a function of tip position. The performance of scanning MFM has been tested by applying the technique to a number of magnetic materials, yielding a resolution of 10 nm and a sensitivity of 10^{-12} N.²²⁻²⁵ This performance places MFM among the most powerful techniques for investigating small magnetic structures. Recently, scanning MFM has been suggested as a possible method for imaging vortex lattices in high- T_c superconductors.²⁶⁻²⁸ Here, we explore another possible application of MFM in the study of superconductivity. Namely, we show that MFM provides a unique tool for determining the London penetration depth of a type-II superconductor.

In the past several years, there have been some scanning tunneling microscope (STM) observations of the Abrikosov flux lattices on the conventional low-temperature superconductors, such as NbSe₂.²⁹ It is well known that STM is a contact probe, and thus requires the samples to have extremely clean surface. For this reason, STM studies on HTS's have mostly failed due to the relatively poor surface characteristics in HTS materials. By contrast, MFM is a noncontact probe, and has been recognized as probably the only method that yields high resolution under ambient conditions without substantial sample preparation, which makes MFM a powerful, universal, and practical noncontact probe technique.³⁰ Its primary advantage for the study of HTS materials with grain boundaries is that we can still treat a single HTS grain as perfect single crystal, since the size of the MFM tip is small relative to the micrometer size (or μ -size) superconducting domains.

In Sec. II, we calculate the magnetostatic interaction between a magnet and a type-II superconductor in the Meissner state, based on the London theory. In the limit of $a/\lambda \gg 1$, we show that the levitation force depends linearly on the penetration depth. Even when $a/\lambda \sim 1$, a simple relationship between the levitation force and the penetration depth still exists for a point dipole magnet. The levitation force between a tiny magnet (or the MFM tip) and a superconductor in the mixed state is presented in Sec. III. In Sec. IV, we derive the expressions of the penetration depth and examine the temperature dependence of the levitation force for different superconducting pairing states. In Sec. V, we show that the intrinsic temperature dependence of the London penetration depth can be determined by MFM through the levitation force measurements. Finally, Sec. VI includes discussions and conclusions.

II. LEVITATION FORCE IN MEISSNER STATE

A. Point dipole model

Let us first consider the levitation force acting on a magnetic point dipole with moment \mathbf{m} placed at a dis-

tance a above a superconductor, as shown in Fig. 1, based on a simple London theory.^{17,18,26} From Maxwell's and London's equations, the vector potential \mathbf{A} can be expressed as

$$\nabla^2 \mathbf{A}(\mathbf{r}) = \mu_0 \mathbf{m} \times \nabla [\delta(x)\delta(y)\delta(z-a)], \quad z > 0, \quad (2.1)$$

$$\nabla^2 \mathbf{A}(\mathbf{r}) - \frac{1}{\lambda^2(T)} \mathbf{A}(\mathbf{r}) = 0, \quad z < 0, \quad (2.2)$$

where μ_0 is the vacuum permeability. The magnetic induction can be calculated by taking the derivative of \mathbf{A} , i.e., $\mathbf{B}(\mathbf{r}) = \nabla \times \mathbf{A}(\mathbf{r})$, and can be written in the form:

$$\mathbf{B}(\mathbf{r}) = \begin{cases} \mathbf{B}_1(\mathbf{r}) + \mathbf{B}_2(\mathbf{r}), & z > 0, \\ \mathbf{B}_3(\mathbf{r}), & z < 0, \end{cases} \quad (2.3)$$

where $\mathbf{B}_1(\mathbf{r})$ is the direct contribution from the point dipole [i.e., the particular solution to Eq. (2.2)], $\mathbf{B}_2(\mathbf{r})$ is the induced field due to the presence of the superconductor, and $\mathbf{B}_3(\mathbf{r})$ is the magnetic field penetrating inside the superconductor. These fields must satisfy the following boundary condition:

$$\mathbf{B}_1(x, y, 0) + \mathbf{B}_2(x, y, 0) = \mathbf{B}_3(x, y, 0). \quad (2.4)$$

Similarly, the vector potential \mathbf{A} can also be written in the form

$$\mathbf{A}(\mathbf{r}) = \begin{cases} \mathbf{A}_1(\mathbf{r}) + \mathbf{A}_2(\mathbf{r}), & z > 0, \\ \mathbf{A}_3(\mathbf{r}), & z < 0. \end{cases} \quad (2.5)$$

By the use of the cylindrical coordinates, it is easy to show that \mathbf{A} has only the θ component $A_\theta(\rho, z)$ due to the symmetry of the problem. The particular solution $A_{1\theta}(\rho, z)$ is easily found,

$$A_{1\theta}(\rho, z) = \frac{\mu_0 m}{4\pi} \frac{\rho}{[\rho^2 + (z-a)^2]^{3/2}}, \quad (2.6)$$

and $A_{2\theta}(\rho, z)$ and $A_{3\theta}(\rho, z)$ satisfy the following equations:

$$\frac{1}{\rho} \frac{\partial}{\partial \rho} \left[\rho \frac{\partial A_{2\theta}}{\partial \rho} \right] + \frac{\partial^2 A_{2\theta}}{\partial z^2} - \frac{1}{\rho^2} A_{2\theta} = 0, \quad (2.7)$$

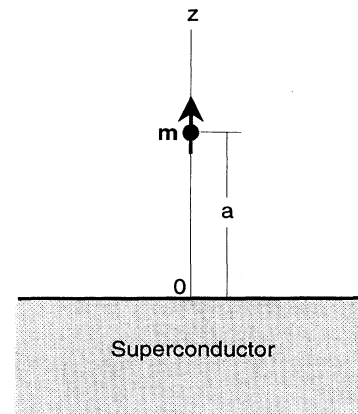


FIG. 1. Diagram of a magnetic point dipole with moment \mathbf{m} placed above a superconductor.

$$\frac{1}{\rho} \frac{\partial}{\partial \rho} \left[\rho \frac{\partial A_{3\theta}}{\partial \rho} \right] + \frac{\partial^2 A_{3\theta}}{\partial z^2} - \frac{1}{\rho^2} A_{3\theta} - \frac{1}{\lambda^2(T)} A_{3\theta} = 0. \quad (2.8)$$

The solutions of $A_{2\theta}$ and $A_{3\theta}$ have the general forms:

$$A_{2\theta} = \int_0^\infty dk C_2(k) e^{-kz} J_1(k\rho), \quad (2.9)$$

$$A_{3\theta} = \int_0^\infty dk C_3(k) e^{\sqrt{k^2+1/\lambda^2(T)}z} J_1(k\rho), \quad (2.10)$$

where $J_n(x)$ is the n th order Bessel function, C_2 and C_3 are determined from the boundary condition (2.4):

$$C_2(k) = \frac{\sqrt{1+k^2\lambda^2(T)} - k\lambda(T)}{\sqrt{1+k^2\lambda^2(T)} + k\lambda(T)} e^{-ka}, \quad (2.11)$$

$$C_3(k) = \frac{2k\lambda(T)}{\sqrt{1+k^2\lambda^2(T)} + k\lambda(T)} e^{-ka}. \quad (2.12)$$

The z component of the induced magnetic field is calculated from $B_{2z} = (1/\rho)A_{2\theta} + \partial A_{2\theta}/\partial \rho$.

$$B_{2z}(\rho, z) = -\frac{\mu_0 m}{4\pi} \int_0^\infty dk k^2 \frac{\sqrt{1+k^2\lambda^2(T)} - k\lambda(T)}{\sqrt{1+k^2\lambda^2(T)} + k\lambda(T)} \times e^{-k(z+a)} J_0(k\rho). \quad (2.13)$$

The self-interaction energy can be written in the form:

$$U = -\frac{1}{2} \mathbf{m} \cdot \mathbf{B}_2(0, a), \quad (2.14)$$

and the levitation force acting on the magnetic dipole can then be obtained from the interaction energy through $F_d = -\partial U/\partial a$:

$$F = \frac{\mu_0 m^2}{64\pi a^4} \times \int_0^\infty dt t^3 e^{-t} \left[1 + \frac{1}{2} \left(\frac{\lambda(T)}{a} \right)^2 t^2 - \frac{\lambda(T)}{a} t \sqrt{1 + 1/4(\lambda(T)/a)^2 t^2} \right]. \quad (2.15)$$

This result gives the exact levitation force for a point magnetic dipole over a superconductor in the sense when the superconductor can be described by the London model. In fact, this force can also be estimated by simulating the field penetrating completely into the superconductor by a layer of thickness equal to the penetration depth λ . In this case, a magnetic dipole is induced in accordance with the potential theory, and the force is given by

$$F = \frac{3\mu_0 m^2}{32\pi [a + \lambda(T)]^4}. \quad (2.16)$$

In the limit of $a/\lambda \gg 1$, both expressions (2.15) and

(2.16) give the same approximate result:

$$F(T) = \alpha - \beta \frac{\lambda(T)}{a}, \quad (2.17)$$

with $\alpha = 3\mu_0 m^2/32\pi a^4$ and $\beta = 4\alpha$. Figure 2 shows the calculated levitation force as a function of a , the separation between the dipole and the superconductor. The solid line represents the result from the London theory [Eq. (2.15)], the dotted line is the linear- λ result from Eq. (2.17). The approximate result from (2.16) is also presented in the figure (dashed line) for comparison. It is seen that all results converge to the linear- λ behavior when the ratio of $a/\lambda > 10$. When $a/\lambda < 10$, there exists a big deviation from the linear- λ result. But, it is clear that the approximation (2.16) is still in good agreement with the London theory (2.15) almost for all range of $a/\lambda > 1$. Thus, in the large a/λ limit, we can estimate the levitation force from the linear- λ approximation in Eq. (2.17), while the approximation (2.16) should be used when $a/\lambda \sim 1$.

B. Shape effect of the magnet

The above calculation is only valid for the simple magnetic dipole model, and does not take the size and geometry of the magnet into account. Here we argue that, in the limit of $a/\lambda \gg 1$, the shape of the magnet only affects the coefficients α and β in Eq. (2.17), but does not change the linear- λ dependence of the levitation force at low temperatures. It can be shown that the levitation force acting on a magnet with arbitrary shape over a type-II superconductor in the Meissner state is given by

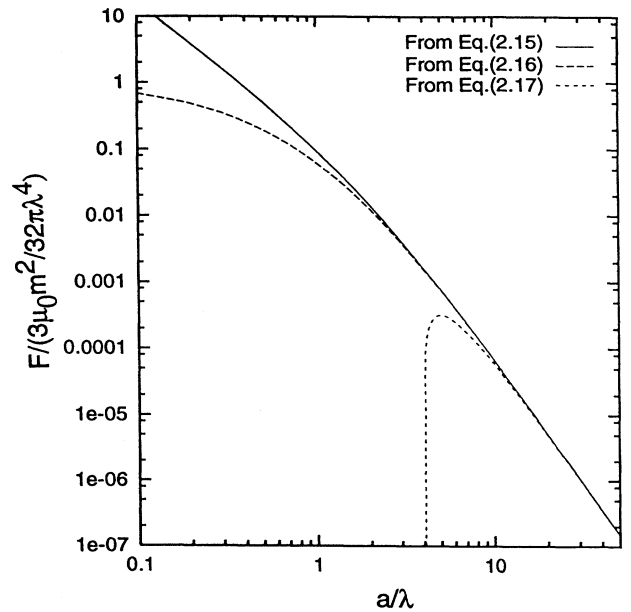


FIG. 2. Levitation force as a function of the separation a between the dipole and the superconductor. Solid line represents the result from the London theory, Eq. (2.15), dashed and dotted lines are the results from the approximations Eqs. (2.16) and (2.17), respectively.

$$F(T) = \frac{\mu_0}{4\pi} \int_0^\infty dk k^3 \frac{\sqrt{1+\lambda^2(T)k^2} - \lambda(T)k}{\sqrt{1+\lambda^2(T)k^2} + \lambda(T)k} e^{-2ak} \int_V d\tau \int_V d\tau' M(\mathbf{r})M(\mathbf{r}') e^{-k(z+z')} J_0[k\sqrt{(x-x')^2+(y-y')^2}], \quad (2.18)$$

where a is the distance between the lower end of the magnet and the superconducting surface, V is the volume of the magnet, $\mathbf{M}(\mathbf{r})$ is the magnetization density distribution of the magnet which is assumed to be polarized along the z direction for simplicity, and the integration for volume elements $d\tau = dx dy dz$ and $d\tau' = dx' dy' dz'$ is carried out over the space distribution of the magnet. Here the origin of the coordinates has been chosen at the lower end of the magnet.

In the limit of $a/\lambda \gg 1$, we can show that the levitation force in Eq. (2.18) is still given by the linear- λ approximation (2.17), but the coefficients α and β have to be replaced by

$$\alpha = \frac{\mu_0}{64\pi a^4} \int_0^\infty dt t^3 e^{-t} \int_V d\tau \int_V d\tau' M(\mathbf{r})M(\mathbf{r}') e^{-t/2a(z+z')} J_0 \left[\frac{t}{2a} \sqrt{(x-x')^2+(y-y')^2} \right], \quad (2.19)$$

$$\beta = \frac{\mu_0}{64\pi a^4} \int_0^\infty dt t^4 e^{-t} \int_V d\tau \int_V d\tau' M(\mathbf{r})M(\mathbf{r}') e^{-t/2a(z+z')} J_0 \left[\frac{t}{2a} \sqrt{(x-x')^2+(y-y')^2} \right]. \quad (2.20)$$

This result means that, in the limit of $a/\lambda \gg 1$, the levitation force between the magnet and the superconductor depends linearly on λ , regardless of the shape of the magnet. Here we list the corresponding coefficients α and β for the homogeneously polarized cylindrical and spherical magnets. The following expressions apply for a cylindrical magnet of moment \mathbf{m} :

$$\alpha = \frac{\mu_0 m^2}{4\pi h^2 R^2} \sum_{i=0}^{\infty} \frac{(-1)^i (2i+1)!(2i+2)!}{i![(i+1)!]^2(i+2)!} \left[\frac{R}{4a+4h} \right]^{2i+2} \left[\left(1 + \frac{h}{a+h} \right)^{-2i-2} + \left(1 - \frac{h}{a+h} \right)^{-2i-2} - 2 \right], \quad (2.21)$$

$$\beta = \frac{\mu_0 m^2}{4\pi h^2 R^2} \sum_{i=0}^{\infty} \frac{(-1)^i [(2i+2)!]^2}{i![(i+1)!]^2(i+2)!} \left[\frac{R}{4a+4h} \right]^{2i+2} \left[\left(1 + \frac{h}{a+h} \right)^{-2i-3} + \left(1 - \frac{h}{a+h} \right)^{-2i-3} - 2 \right], \quad (2.22)$$

where $2h$ is the height and R is the radius. For a spherical magnet of radius R and moment \mathbf{m} , the coefficients are found to be given as follows:

$$\alpha = \frac{9\mu_0 m^2}{4\pi R^4} \sum_{i,j=1}^{\infty} \left[\frac{R}{2a+2R} \right]^{2i+2j} \sum_{k=0}^{\infty} (-1)^k \left[\frac{R}{8a+8R} \right]^{2k} C_{ijk}^{-1}, \quad (2.23)$$

$$\beta = \frac{9\mu_0 m^2}{4\pi R^4} \sum_{i,j=1}^{\infty} \left[\frac{R}{2a+2R} \right]^{2i+2j} \sum_{k=0}^{\infty} (-1)^k \left[\frac{R}{8a+8R} \right]^{2k} C_{ijk}^0. \quad (2.24)$$

Here the magnets have been assumed to be polarized in the levitation direction. The constants C_{ijk}^μ in Eqs. (2.23) and (2.24) are defined by

$$C_{ijk}^\mu = \frac{(2i+2j+2k+\mu)!(i+j+2k+1)!}{k!(i+j+k+1)!(2i+2k+1)!(2j+2k+1)!}. \quad (2.25)$$

In the limit as h and R approach zero, it is easy to show that the results of cylindrical [Eqs. (2.21) and (2.22)] and spherical [Eqs. (2.23) and (2.24)] magnets reduce back to those for a magnetic point dipole, Eq. (2.17), as expected. The above results for cylindrical and spherical magnets indicate that, at the lowest order of approximation, a magnet of any shape can be treated as a simple magnetic point dipole. At low temperatures, although the size and geometry of the magnet strongly affect the coefficients, they do not alter the simple linear relation between levitation force and penetration depth in the limit of $a/\lambda \gg 1$. Therefore, it is possible to determine the London penetration depth directly from measurements of the levitation force, regardless of the shape of the magnet used in the experiment.

C. Shape effect of the superconductor

In all the above calculations, the superconductor is assumed to fill half of the infinite space. In fact, for practical measurements, the superconducting samples have their size and geometry. Here we study a simple case, i.e., a point dipole over a superconducting thin film with a finite thickness d . We examine the thickness dependence of the levitation force in the Meissner state. In this case, above the superconducting film ($z > d/2$, here the origin of the z axis is chosen at the center of the film), Maxwell's equation (2.1) is still valid. Inside the film ($-d/2 < z < d/2$), the electrodynamics is described by London's equation (2.2). Below the film ($z < -d/2$), the vector potential satisfies the Laplace's equation:

$$\nabla^2 \mathbf{A}(\mathbf{r}) = 0. \quad (2.26)$$

The problem then reduces to solve Eqs. (2.1), (2.2), and (2.26) under the continuous condition of \mathbf{B} at the

boundaries.³¹ Following the similar procedure as we did in the case of the half infinite superconductor, we find the levitation force acting on a point dipole placed above the superconducting film to be given by

$$F = \frac{\mu_0 m^2}{64\pi a^4} \int_0^\infty dt t^3 e^{-t} \left[1 + \frac{t^2 \lambda^2}{2a^2} + \frac{t\lambda}{a} \sqrt{1 + (t^2 \lambda^2 / 4a^2)} \coth \left(\frac{d}{\lambda} \sqrt{1 + t^2 \lambda^2 / 4a^2} \right) \right]^{-1}. \quad (2.27)$$

It is seen that, when the thickness of the film $d \rightarrow \infty$, the above result reduces back to Eq. (2.15), as expected. In the limit of $a/\lambda \gg 1$, we find

$$F = \alpha - \beta \left(\frac{\lambda}{a} \right) \coth \left(\frac{d}{\lambda} \right), \quad (2.28)$$

where α and β are the same as those given in Eq. (2.17). Figure 3 shows the thickness dependence of the levitation force for a magnetic point dipole model with a fixed distance $a/\lambda = 1$ (solid line) and 100 (dashed line). It is clear that, in the smaller a case, the thickness of the film has a larger effect on the levitation force. The levitation force has reached about 95% for $a/\lambda = 1$ and 99% for $a/\lambda = 100$ of its saturation value when the thickness is equal to the penetration depth, and quickly increases close to its saturation value when the thickness is larger than the penetration depth. From a physical point of view, λ indeed shows an effective measure of the depth to which the magnetic field from the magnet can penetrate. Namely, when $d < \lambda$, the magnetic field can leak into the superconducting thin film, which results in a significant reduction of the levitation force. On the other hand, when $d > \lambda$, the thin film can effectively block the transmission of the magnetic field, which leads to an increase in levitation force. In practice, the thickness of the superconducting film is usually larger than the penetration depth. Therefore, the thickness dependence

of the levitation force may be neglected. Otherwise, Eq. (2.27), or its approximation (2.28) in the limit of $a/\lambda \gg 1$, has to be used to calculate the levitation force.

III. LEVITATION FORCE IN MIXED STATE

In this section, we calculate the levitation force acting on a magnet over a type-II superconductor in the mixed state. Here we consider a simple case, i.e., the applied magnetic field H is very close to the lower critical field H_{c1} ($H_{c1} \leq H \ll H_{c2}$ with H_{c2} being the upper critical field) and only one flux line exists in the superconductor near the bottom of the tiny magnet (or the MFM tip). Generalization to the case with more flux lines is straightforward. In this case, the force acting on the magnet (or the MFM tip) includes two parts: one is due to the shielding field caused by the magnet itself (Meissner effect), and the other is due to the presence of the flux line. Both of them can be analyzed within the London framework of vortex lines in type-II superconductors, assuming a normal core of radius roughly equal to the coherence length ξ . If $H_{c1} \leq H \ll H_{c2}$, this model is valid almost in entire temperature region below T_c in the limit $\kappa = \lambda/\xi \gg 1$, or when the radius of the vortex core is very small.

Let us consider the simplest case, i.e., a point dipole is placed just over the flux line. In this case, inside the superconductor, the London equation (2.2) has to be replaced by³²

$$\nabla^2 \mathbf{B}(\mathbf{r}) - \frac{1}{\lambda^2(T)} \mathbf{B}(\mathbf{r}) = -\frac{\phi_0}{\lambda^2(T)} \hat{z} \delta(x) \delta(y), \quad z < 0. \quad (3.1)$$

Where ϕ_0 is the flux quantum. Above the superconductor, Maxwell's equation (2.1) is still valid. In order to solve Eqs. (3.1) and (2.1) under the boundary condition (2.4), it is convenient to write \mathbf{B} in the form:

$$\mathbf{B}(\mathbf{r}) = \begin{cases} \mathbf{B}_1(\mathbf{r}) + \mathbf{B}_2(\mathbf{r}), & z > 0 \\ \mathbf{B}_3(\mathbf{r}) + \mathbf{B}_4(\mathbf{r}), & z < 0, \end{cases} \quad (3.2)$$

where $\mathbf{B}_1(\mathbf{r})$ and $\mathbf{B}_3(\mathbf{r})$ are, respectively, the particular solutions of Eqs. (2.1) and (3.1):

$$\mathbf{B}_1(\mathbf{r}) = \frac{\mu_0 m}{4\pi} \left\{ \frac{3\rho(z-a)}{[\rho^2 + (z-a)^2]^{5/2}} \hat{\rho} + \frac{2(z-a)^2 - \rho^2}{[\rho^2 + (z-a)^2]^{5/2}} \hat{z} \right\}, \quad (3.3)$$

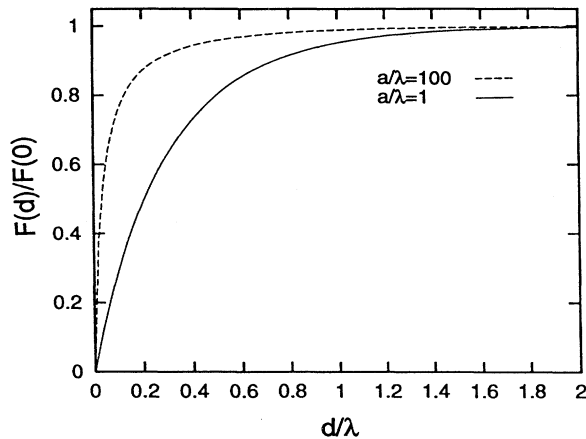


FIG. 3. Thickness dependence of the levitation force between a magnetic dipole and a superconducting thin film for $a/\lambda = 1$ (solid line) and 100 (dashed line).

$$\mathbf{B}_3(\mathbf{r}) = \frac{\phi_0}{2\pi\lambda} K_0 \left[\frac{\rho}{\lambda} \right] \hat{\mathbf{z}}, \quad (3.4)$$

where $K_0(x)$ is the zeroth-order Bessel function of the imaginary argument. The general solutions of Eqs. (2.1) and (3.1) have the forms:

$$\mathbf{B}_2(\mathbf{r}) = \int_0^\infty dk k D_2(k) e^{-kz} [J_1(k\rho)\hat{\rho} + J_0(k\rho)\hat{\mathbf{z}}], \quad (3.5)$$

$$\mathbf{B}_4(\mathbf{r}) = \int_0^\infty dk k D_4(k) e^{\sqrt{k^2+1/\lambda^2}z} \times \left[-\sqrt{1+1/k^2\lambda^2} J_1(k\rho)\hat{\rho} + J_0(k\rho)\hat{\mathbf{z}} \right]. \quad (3.6)$$

From the boundary condition (2.4), we find

$$D_2(k) = -\frac{1}{2\pi} \frac{k\lambda}{\sqrt{1+k^2\lambda^2} + k\lambda} \times \left[\frac{\mu_0 m}{2} e^{-ka} \left[\sqrt{k^2+1/\lambda^2} - k \right] - \frac{\phi_0}{k\lambda\sqrt{1+k^2\lambda^2}} \right], \quad (3.7)$$

$$D_4(k) = \frac{1}{2\pi} \frac{k\lambda}{\sqrt{1+k^2\lambda^2} + k\lambda} \times \left[\mu_0 m k e^{-ka} \left[\sqrt{k^2+1/\lambda^2} - k \right] - \frac{\phi_0}{1+k^2\lambda^2} \right]. \quad (3.8)$$

Then the levitation force acting on the magnetic dipole is given by

$$\mathbf{F} = \mathbf{F}_1 + \mathbf{F}_2 = \frac{1}{2} \frac{\partial}{\partial a} [\mathbf{m} \cdot \mathbf{B}_2(0, a)], \quad (3.9)$$

where F_1 is exactly the same as that given in Eq. (2.15), caused by the magnet itself (Meissner effect), while F_2 , caused by the flux line, is found to be

$$F_2(T) = -\frac{\phi_0 m}{2\pi} \int_0^\infty dk \frac{k^2 e^{-ka}}{1+k^2\lambda^2(T) + k\lambda(T)\sqrt{1+k^2\lambda^2(T)}}. \quad (3.10)$$

In the limit of $a/\lambda \gg 1$, we find

$$F_2 = -\alpha' + \beta' \frac{\lambda(T)}{a}, \quad (3.11)$$

where $\alpha' = m\phi_0/\pi$, and $\beta' = 3\alpha'$. This result indicates that, in the limit of $a/\lambda \gg 1$, we can still obtain a linear- λ dependence of the levitation force as given in Eq. (2.18), but the λ -independent coefficients α and β are modified to $\alpha - \alpha'$ and $\beta - \beta'$. Namely, the presence of the pinned flux line only decreases the strength of the levitation force, it does not alter its linear- λ dependence.

For a magnet with an arbitrary shape, we find

$$F_2(T) = -\frac{\phi_0 m}{2\pi} \int_0^\infty dk \frac{k^2 e^{-ka}}{1+k^2\lambda^2(T) + k\lambda(T)\sqrt{1+k^2\lambda^2(T)}} \times \int_V d\tau M(\mathbf{r}) e^{-kz} J_0 \times [k\sqrt{(x-x_0)^2 + (y-y_0)^2}], \quad (3.12)$$

where (x_0, y_0) is the location of the flux line. Again, in the $a/\lambda \gg 1$ limit, a linear- λ dependent levitation force as given in Eq. (3.11) can be obtained, but with

$$\alpha' = \frac{\phi_0 m}{2\pi a^2} \int_0^\infty dt t^2 e^{-t} \times \int_V d\tau M(\mathbf{r}) e^{-tz/a} J_0 \times \left[\frac{t}{a} \sqrt{(x-x_0)^2 + (y-y_0)^2} \right], \quad (3.13)$$

$$\beta' = \frac{\phi_0 m}{2\pi a^2} \int_0^\infty dt t^3 e^{-t} \times \int_V d\tau M(\mathbf{r}) e^{-tz/a} J_0 \times \left[\frac{t}{a} \sqrt{(x-x_0)^2 + (y-y_0)^2} \right]. \quad (3.14)$$

IV. PENETRATION DEPTH AND LEVITATION FORCE FOR DIFFERENT PAIRING STATES

From the above calculations, we see that the temperature dependence of the levitation force originates completely from the penetration depth, which implies that the temperature dependence of the levitation force contains the same amount of information as that of the penetration depth. It is well known that the temperature dependence of $\lambda(T)$ is different for different pairing symmetries. We now present results for three particular pairing states, which are currently of interest in the study of high- T_c superconductivity, i.e., (i) s wave with a constant gap function Δ_s , (ii) d wave with a gap function $\Delta_d(\mathbf{k}) = \Delta_d(\hat{k}_x^2 - \hat{k}_y^2) = \Delta_d \cos 2\phi$, and (iii) $s + id$ state with a gap function $\Delta_{s+id}(\mathbf{k}) = \Delta_s + i\Delta_d \cos 2\phi$.³³ Here, we have chosen to work with a BCS weak-coupling superconductor and a cylindrical Fermi surface¹² for simplicity.

In order to determine the penetration depth, we calculate the electromagnetic response tensor \mathbf{K} , relating the current density \mathbf{j} to an applied vector potential \mathbf{A} : $\mathbf{j} = -\mathbf{K} \mathbf{A}$. If the K_{ij} is diagonal, it is simply related to the eigenvalues of the penetration depth: $(4\pi/c)K_{ii} = \lambda^{-2}$, where λ is the penetration depth for current flow in the i direction. In the BCS-like model for an anisotropic superconductor, the response tensor is given by

$$K_{ij} = \frac{e^2}{c} \left\langle v_i(k) v_j(k) \int_0^\infty d\omega \tanh \frac{\omega}{2T} \operatorname{Re} \frac{\Delta_k^2}{(\omega^2 - \Delta_k^2)^{3/2}} \right\rangle, \quad (4.1)$$

where $\langle \dots \rangle$ represents an angular average over the Fermi surface, and $\mathbf{v}(\mathbf{k})$ is the Fermi velocity. For a general $s + id$ gap function $\Delta_{s+ik}(k)$, we find

$$\left[\frac{\lambda(0)}{\lambda(T)} \right]^2 = 1 - \frac{4}{\pi T} \left[\int_{\Delta_s}^{\sqrt{\Delta_s^2 + \Delta_d^2}} d\omega \frac{e^{\omega/T}}{(1+e^{\omega/T})^2} \frac{\omega}{\Delta_d} K \left[\frac{\sqrt{\omega^2 - \Delta_s^2}}{\Delta_d} \right] + \int_{\sqrt{\Delta_s^2 + \Delta_d^2}}^{\infty} d\omega \frac{e^{\omega/T}}{(1+e^{\omega/T})^2} \frac{\omega}{\sqrt{\omega^2 - \Delta_s^2}} K \left[\frac{\Delta_d}{\sqrt{\omega^2 - \Delta_s^2}} \right] \right], \quad (4.2)$$

where $K(x)$ is the complete elliptic integral of the first kind and $\lambda(0)$ is the value of the penetration depth at zero temperature. If we set $\Delta_d=0$, the above equation reduces to the conventional s -wave result¹

$$\left[\frac{\lambda(0)}{\lambda(T)} \right]^2 = 1 - \frac{2}{T} \int_{\Delta_s}^{\infty} d\omega \frac{e^{\omega/T}}{(1+e^{\omega/T})^2} \frac{\omega}{\sqrt{\omega^2 - \Delta_s^2}}. \quad (4.3)$$

On the other hand, Eq. (4.2) gives the pure d -wave result if we put $\Delta_s=0$:

$$\left[\frac{\lambda(0)}{\lambda(T)} \right]^2 = 1 - \frac{4}{\pi T} \left[\int_0^{\Delta_d} d\omega \frac{e^{\omega/T}}{(1+e^{\omega/T})^2} \frac{\omega}{\Delta_d} K \left[\frac{\omega}{\Delta_d} \right] + \int_{\Delta_d}^{\infty} d\omega \frac{e^{\omega/T}}{(1+e^{\omega/T})^2} K \left[\frac{\Delta_d}{\omega} \right] \right]. \quad (4.4)$$

In order to find the temperature dependence of the penetration depth, or of the levitation force, one must also know the temperature dependence of the gap functions. In our calculation, we use the standard approximation from Ref. 1

$$\Delta_s(T) = \Delta_s(0) \tanh(1.74\sqrt{T_c/T-1}), \quad (4.5)$$

which fits the numerical solution of the weak-coupling BCS gap function very well. The temperature dependence of the d -wave gap function should be determined from the gap equation³⁴

$$\gamma^{-1} = 2\pi T \langle |f|^2 \rangle \sum_{\omega_n} \left\langle \frac{|f|^2}{\sqrt{\omega_n^2 + \Delta_d^2} |f|^2} \right\rangle, \quad (4.6)$$

with $f = \cos 2\phi$ and γ is the dimensionless coupling constant, ω_n is the Matsubara frequency and the sum over ω_n is cutoff at $\omega_n = \epsilon_c$. The gap equation (4.6) has been solved recently by Won and Maki,³⁴ and $\Delta_d(T)/\Delta_d(0)$ (solid line) is shown in Fig. 4 as a function of T/T_c together with $\Delta_s(T)/\Delta_s(0)$ (dotted line) for the s -wave superconductor. We see from the figure that $\Delta_d(T)/\Delta_d(0)$ behaves basically similar to the s -wave one. Therefore, we may also use the same formula (4.5) for $\Delta_d(T)$ for simplicity. When $T \rightarrow 0$, we can find analytic expressions for pure s wave and d wave

$$\frac{\lambda(T)}{\lambda(0)} = \begin{cases} 1 + \sqrt{\pi \Delta_s(0)/2T} e^{-\Delta_s(0)/T} & \text{for } s \text{ wave,} \\ 1 + 0.693T/\Delta_d(0) & \text{for } d \text{ wave.} \end{cases} \quad (4.7)$$

This means that, at low temperatures, $\lambda(T)$ depends exponentially on T for the s wave, while it has a linear- T dependence for the d wave.

Figures 5(a) and 5(b) show $\lambda(T)$ as functions of T and T^2 , respectively, for the s -wave (dotted line), d -wave (dot-dashed line), and $s + id$ states (solid line). It is obvious from the figure that the penetration depth shows a T^2 dependence in a wide low-temperature range for an $s + id$ state with a dominant d -wave component [in this calculation, $\Delta_s(0)/\Delta_d(0)=0.2$ is used]. This result provides an alternative explanation for the T^2 dependence of λ , observed in high-quality single crystals of Bi-Sr-Ca-Cu-O and Y-Ba-Cu-O thin films by Ma *et al.*¹⁰ It can be understood that the high- T_c superconductors are in the $s + id$ state with a small s -wave component. At high temperatures, the d -wave component dominates the thermodynamic properties, while the small s -wave component becomes important at very low temperatures ($T \rightarrow 0$). The crossover between the d wave and s wave in a wide low-temperature range gives a T^2 dependence of λ , in agreement with the experimental observations.¹⁰ More remarkably, at very low temperatures, our result shows a deviation from T^2 towards an exponential temperature dependence due to the existence of a small s -wave component. Such a fine structure at very low temperatures was also observed experimentally.¹⁰ Ma *et al.* noted that

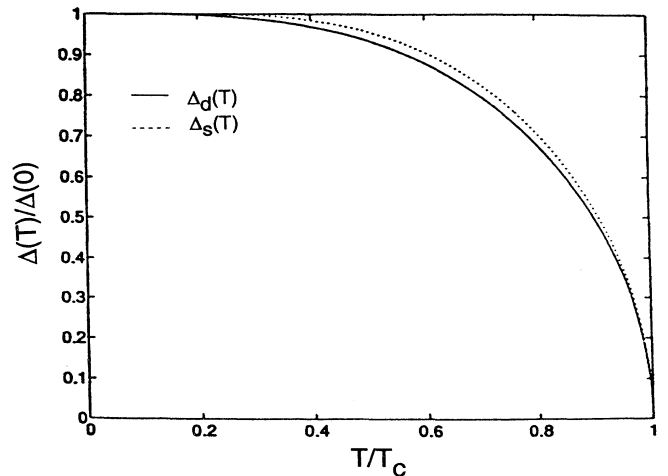


FIG. 4. The superconducting gap function as a function of temperature. Here the solid line is for d wave and the dotted line for s wave.

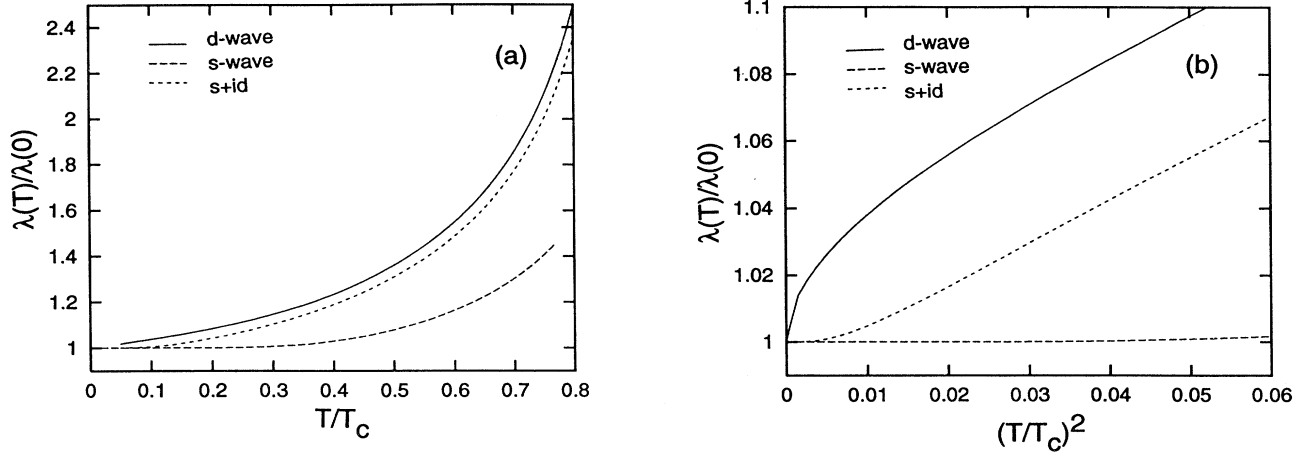


FIG. 5. Penetration depth as functions of T (a) and T^2 (b) for d -wave (solid line), s -wave (dashed line), and for the $s + id$ state with $\Delta_s(0)/\Delta_d(0)=0.2$ (dotted line).

the temperature dependence of $\lambda(T)$ is T^2 for all samples used in their experiment, except at lowest temperatures, where there is a deviation towards a flatter temperature dependence. Quantitative analysis shows that these deviations can be viewed as a crossover to an activated behavior with a small gap, in agreement with the $s + id$ state. Previously, it has been pointed out that for a d -wave superconductor, the strong impurity scattering (unitarity limit) could change the linear- T dependence of λ to T^2 .¹²

Now the temperature-dependent levitation force can be calculated by substituting the expressions for $\lambda(T)$, given in Eqs. (4.2)–(4.4), for the $s + id$, s -wave, and d -wave

states, into Eq. (2.18) in the Meissner state, or into Eq. (3.12) in the mixed state. At low temperatures, the asymptotic behavior of the levitation force acting on a magnet with arbitrary shape in the Meissner state for pure s - and d -wave states can be obtained from Eqs. (2.18) and (4.7):

$$F(T) = \begin{cases} A - B\sqrt{\pi\Delta_s(0)/2T} e^{-\Delta_s(0)/T} & \text{for } s \text{ wave,} \\ A - 0.693BT/\Delta_d(0) & \text{for } d \text{ wave,} \end{cases} \quad (4.8)$$

where A and B are temperature-independent constants:

$$A = \frac{\mu_0}{4\pi\lambda^4(0)} \int_0^\infty dt t^3 \frac{\sqrt{1+t^2}-t}{\sqrt{1+t^2}+t} e^{-2at/\lambda(0)} \times \int_V d\tau \int_V d\tau' M(\mathbf{r})M(\mathbf{r}') e^{-t/\lambda(0)(z+z')} J_0 \left[\frac{t}{\lambda(0)} \sqrt{(x-x')^2+(y-y')^2} \right], \quad (4.9)$$

$$B = \frac{\mu_0}{2\pi\lambda^4(0)} \int_0^\infty dt \frac{t^4}{\sqrt{1+t^2}} \frac{\sqrt{1+t^2}-t}{\sqrt{1+t^2}+t} e^{-2at/\lambda(0)} \times \int_V d\tau \int_V d\tau' M(\mathbf{r})M(\mathbf{r}') e^{-t/\lambda(0)(z+z')} J_0 \left[\frac{t}{\lambda(0)} \sqrt{(x-x')^2+(y+y')^2} \right]. \quad (4.10)$$

These results show that, at low temperatures, the levitation force depends linearly on temperature for the d wave, while it varies exponentially with temperature for the s wave, regardless of the shape of the magnet.

Figure 6 shows the calculated levitation force for a point dipole model with $a/\lambda(0)=1$ (a) and 100 (b). We see from the figure that the difference in the temperature dependence of the levitation force between s -wave and d -wave superconductors extends over almost the entire temperature region below T_c . In addition, we find that,

the closer the magnet is to the surface of the superconductor, the larger the difference. The levitation force versus T^2 is plotted in Fig. 7 for different pairing states with $a/\lambda(0)=1$ (a) and 100 (b). A nice T^2 dependence of the levitation force is found for the $s + id$ state, regardless of the separation between the magnet and the superconductor. Thus the low-temperature behavior of the levitation force is very similar to that of the London penetration depth. Therefore, one may distinguish between the different possible symmetries of the pairing state by

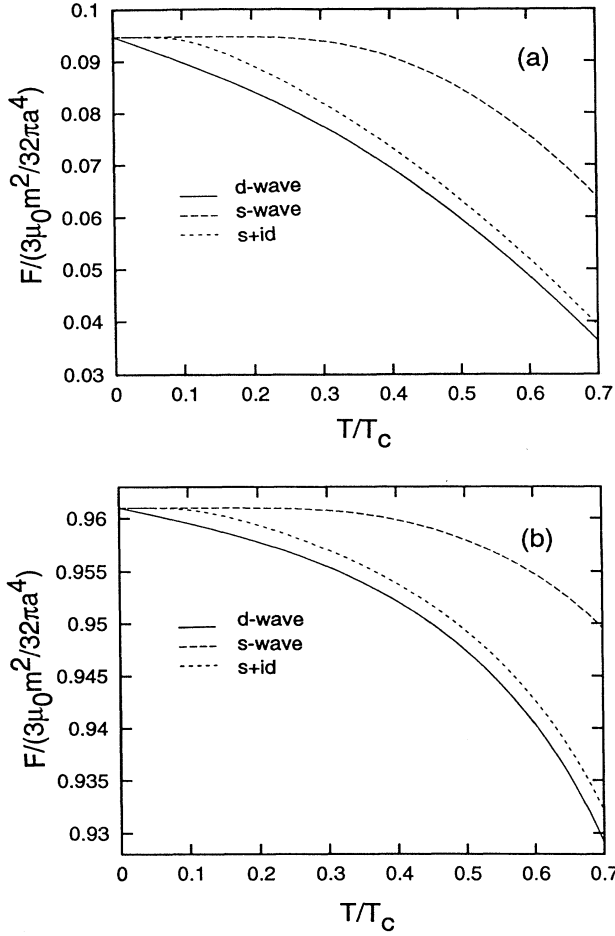


FIG. 6. Levitation force versus temperature for a magnetic dipole model with $a/\lambda(0)=1$ (a) and 100 (b). The different curves represent the results for different pairing states. For the $s+id$ state, the ratio of $\Delta_s(0)/\Delta_d(0)=0.2$

directly examining the temperature dependence of the levitation force.

V. USE OF MFM TO DETERMINE PENETRATION DEPTH

In the previous sections, we have calculated the levitation force, and have found that there exists a simple relationship between the levitation force and the penetration depth. From such a simple relation, it is possible to determine the penetration depth directly from the levitation force measurements. Thus, the problem now becomes how one can *accurately* measure the levitation force. As mentioned in the introduction, MFM has been recognized as probably the only method that yields high resolution under ambient conditions without substantial sample preparation, which makes MFM a powerful, universal, and practical noncontact probe technique.³⁰ Its primary advantage for the study of HTS materials with grain boundaries is that we can still treat a single HTS grain as perfect single crystal, since the size of the

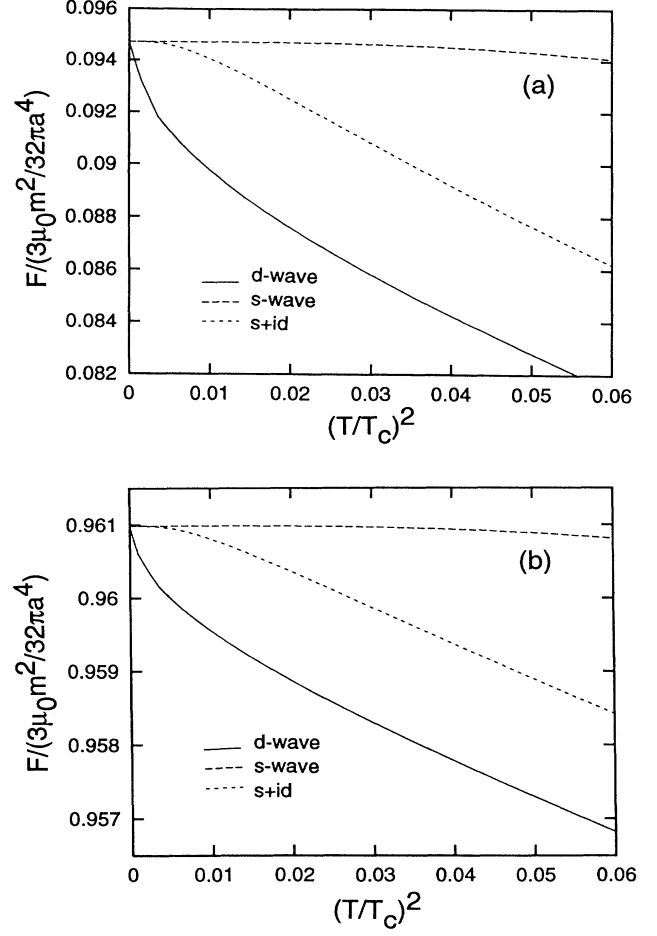


FIG. 7. Levitation force versus T^2 for a magnetic dipole model with $a/\lambda(0)=1$ (a) and 100 (b). The different curves represent the results for different pairing states. For the $s+id$ state, the ratio of $\Delta_s(0)/\Delta_d(0)=0.2$ is used.

MFM tip is small relative to the micrometer size (or μ -size) superconducting domains. In fact, the *intrinsic* temperature dependence of the magnetic levitation force between the tip and the superconductor may be determined by the following steps:

- (i) scan a superconducting surface by MFM or STM (Ref. 35) and select an appropriate μ -size superconducting domain which we are going to study;
- (ii) place the magnetic tip of the MFM at the center of the domain;
- (iii) measure the levitation force as a function of temperature.

This procedure enables one to avoid the effects of grain boundaries and related imperfections on our *microscopic* measurements of the magnetic levitation force, by contrast to *macroscopic* experiments, where grain boundaries and inhomogeneities have a strong effect on the results. We will show in the following discussions that the intrinsic levitation force of a single grain can be used to determine the London penetration depth. For simplicity, we use a magnetic point dipole model to simulate the MFM

tip, and only present the result in the Meissner state. The generalization to the case where the tip has arbitrary shape and the superconductor is in the mixed state is straightforward.

The principle of the MFM operation is that there exists a levitation force acting on the MFM tip integrated with a cantilever placed close to the center of the selected superconducting domain. The cantilever on which the tip is mounted will bend upwards due to such a magnetic levitation force, this deflection is detected, and the levitation force exerted on the lever can then be calculated from Eq. (2.15) for a point dipole tip. We now estimate the range of the levitation force from Eq. (2.15) for a conventional, well-studied superconductor NbSe₂ with a penetration depth $\lambda = 69$ nm.²⁹ For simplicity, we consider a Fe tip of a spherical shape with a radius of 200 nm, and take $a = 1000$ nm. The levitation force is found to be about 10^{-10} N. While for a typical HTS material, this force reduces to $\sim 10^{-11}$ N because this material has a larger λ . It is clear that the levitation force is well in the range of the MFM sensitivity. Therefore, the MFM can be used to *accurately* determine the temperature-dependent levitation force. We have shown in Sec. II that, when the separation between the tip and the superconductor is comparable with the penetration depth, we can use the approximation (2.16); while the linear- λ approximation (2.17) is applicable for $a/\lambda \gg 1$. As long as the levitation force is measured by the MFM, the temperature-dependent penetration depth at low temperatures can readily be determined from the following relation:

$$\frac{\lambda(T)}{\lambda(0)} = \begin{cases} \left[\frac{F(0)}{F(T)} \right]^{1/4} \left[1 + \frac{a}{\lambda(0)} \right] - \frac{a}{\lambda(0)}, & a > \lambda(0) \\ \frac{1}{4} \left[\frac{a}{\lambda(0)} - \left(\frac{a}{\lambda(0)} - 4 \right) \frac{F(T)}{F(0)} \right], & a \gg \lambda(0). \end{cases} \quad (5.1)$$

Finally, we should point out that the difficulty of quantitatively determining temperature dependence of the levitation force using MFM is the measurement and stabilization of the sample-tip separation. There are a number of causes of unwanted fluctuations in the sample-tip separation, the most significant being differential contraction due to changes in temperature. In response to this problem, fortunately, a new technique, called optically stabilized double-interferometer technique,³⁶ has been developed. This approach allows the sample-probe spacing to be held constant or varied in a quantitative manner during data acquisition. Therefore, it is possible to realize our theoretical results in the laboratory using MFM by incorporating this optical technique.

VI. DISCUSSIONS AND CONCLUSIONS

We have calculated the levitation force acting on a magnet placed above a type-II superconductor with different pairing symmetries in both the Meissner and mixed states. To our knowledge, this is the first attempt to relate the magnetic levitation force to the supercon-

ducting pairing state. Our main results include two parts. First, we have examined the temperature dependences of both the London penetration depth and levitation force for various pairing symmetries including s -wave, d -wave, and $s + id$ states. We have shown that the temperature dependence of the levitation force and penetration depth is different for different pairing states. One may distinguish between the different possible symmetries of the pairing states by directly examining the temperature-dependent levitation force. We have found that, for the conventional s wave, both of the penetration depth and levitation force have an exponential temperature dependence due to the presence of an energy gap. While for the d wave, they show a linear- T dependence. In particular, for the $s + id$ state with a dominant d -wave component, a T^2 dependence in a wide low-temperature range has been obtained. This result may provide an alternative explanation for the T^2 dependence of λ , observed in high- T_c superconductors, if the HTS materials are assumed to be in the $s + id$ state with a small s -wave component. Of course, one cannot rule out that the T^2 dependence of λ may also be accounted for by a proper anisotropic pairing state.

Secondly, we have found a simple relationship between the levitation force and the London penetration depth. In the limit of $a/\lambda > 10$, the levitation force varies linearly with the penetration depth, regardless of the shape of the magnet. We have also studied the thickness effect on the levitation force between the magnet and the superconducting thin film, and have shown that the thickness effect on the levitation force can be neglected if the thickness of the film is larger than the penetration depth. These results provide a method of measuring the London penetration depth, namely, one can determine λ directly from the levitation force measurements. In order to realize our method in the laboratory, we have proposed that the temperature-dependent levitation force can accurately be measured using MFM. The microscopic size of the MFM tip and the noncontact feature of the MFM enable us to obtain the intrinsic temperature-dependent levitation force of a single grain, regardless of the overall quality of the superconducting sample. In the past, Abrikosov flux lattices have been successfully observed using STM in the conventional low-temperature superconductors, such as NbSe₂. It is well known that STM is a contact probe, and thus requires the samples to have extremely clean surface. For this reason, STM studies on HTS have mostly failed due to the relatively poor surface characteristics in HTS materials. Instead, the noncontact MFM provides a unique tool for study of the HTS materials.

We have emphasized the microscopic character of MFM that makes it possible to avoid the effects of grain boundaries and related sample imperfections on the intrinsic temperature dependence of the penetration depth. The advantage of the present method is clear in comparison with the macroscopic approach, such as microwave technique. Macroscopic methods only measure the effective averaged penetration depth. The presence of the grain boundaries and other imperfections in HTS materials leads to difficulties in directly observing their fundamental physics properties by macroscopic methods.

ACKNOWLEDGMENTS

This research was supported by the Robert A. Welch Foundation, and by the State of Texas through the Texas Center for Superconductivity at University of Houston, the Advanced Research Program, and the Advanced Technology Program.

-
- ¹B. Muhlschlegel, *Z. Phys.* **155**, 313 (1959).
²C. Gros, R. Joynt, and T. M. Rice, *Z. Phys. B* **68**, 425 (1987).
³Z. Y. Weng, T. K. Lee, and C. S. Ting, *Phys. Rev. B* **38**, 6561 (1988).
⁴P. Mouthoux, A. V. Balatsky, and D. Pines, *Phys. Rev. Lett.* **67**, 3448 (1991).
⁵J. Annett, N. Goldenfeld, and S. R. Penn, *Phys. Rev. B* **43**, 2778 (1991).
⁶D. Einzel, P. J. Hirschfeld, F. Gross, B. S. Chandrasekhar, K. Andres, H. R. Ott, J. Beuers, Z. Fisk, and J. L. Smith, *Phys. Rev. Lett.* **56**, 2513 (1986).
⁷F. Gross, B. S. Chandrasekhar, K. Andres, U. Rauchschwalbe, and E. B. Bucher, *Physica C* **153-155**, 439 (1988).
⁸A. T. Fiory, A. F. Hebard, P. M. Mankiewich, and R. E. Howard, *Phys. Rev. Lett.* **61**, 1419 (1988).
⁹W. N. Hardy, D. A. Bonn, D. C. Morgan, R. Liang, and K. Zhang, *Phys. Rev. Lett.* **70**, 3999 (1993).
¹⁰Z. Ma, R. C. Taber, L. W. Lombardo, A. Kapitulnik, M. R. Beasley, P. Merchant, C. B. Eom, S. Y. Hou, and J. M. Phillips, *Phys. Rev. Lett.* **71**, 781 (1993).
¹¹N. Klein, N. Tellmann, H. Schulz, K. Urban, S. A. Wolf, and V. Z. Kresin, *Phys. Rev. Lett.* **71**, 3355 (1993).
¹²P. J. Hirschfeld and N. Goldenfeld, *Phys. Rev. B* **48**, 4219 (1993).
¹³P. J. Hirschfeld, W. O. Putikka, and D. J. Scalapino, *Phys. Rev. Lett.* **71**, 3705 (1993).
¹⁴M. Prohammer and J. Carbotte, *Phys. Rev. D* **43**, 5370 (1991).
¹⁵D. A. Bonn, P. Dosanjh, R. Liang, and W. N. Hardy, *Phys. Rev. Lett.* **68**, 2390 (1992).
¹⁶F. C. Moon, M. M. Yanoviak, and R. Ware, *Appl. Phys. Lett.* **52**, 1534 (1988).
¹⁷Z. J. Yang, T. H. Johansen, H. Bratsberg, A. Bhatnagar, and A. T. Skjeltorp, *Physica C* **197**, 136 (1992).
¹⁸Z. J. Yang, *Jpn. J. Appl. Phys.* **31**, L477 (1992).
¹⁹Y. Martin and K. K. Wickramasinghe, *Appl. Phys. Lett.* **50**, 1455 (1987).
²⁰J. J. Saenz, N. Garcia, P. Grutter, E. Meyer, H. Heinzelmann, R. Wiesendanger, L. Rosenthaler, H. R. Hidber, and H. J. Güntherodt, *J. Appl. Phys.* **62**, 4293 (1987).
²¹G. Binnig, C. F. Quate, and Ch. Gerber, *Phys. Rev. Lett.* **56**, 930 (1986).
²²U. Hartmann, *Phys. Rev. B* **40**, 7421 (1989).
²³P. C. D. Hobbs, D. W. Abraham, H. K. Wickramasinghe, *Appl. Phys. Lett.* **55**, 2357 (1989).
²⁴A. J. Den Boef, *Appl. Phys. Lett.* **56**, 2045 (1990).
²⁵P. Grütter, A. Wadas, E. Meyer, H. Heinzelmann, H. R. Hidber, H. J. Güntherodt, *J. Vac. Sci. Technol. A* **8**, 406 (1990).
²⁶H. J. Hug, Th. Jung, H. J. Güntherodt, and H. Thomas, *Physica C* **175**, 357 (1991).
²⁷R. Berthe, U. Hartmann, and C. Heiden, *Appl. Phys. Lett.* **57**, 2351 (1990).
²⁸A. Wadas, O. Fritz, H. J. Hug, and H. C. Güntherodt, *Z. Phys. B* **88**, 317 (1992).
²⁹H. F. Hess, R. B. Robinson, R. C. Dynes, J. M. Valles, Jr., and J. V. Waszczak, *Phys. Rev. Lett.* **62**, 214 (1989); H. F. Hess, R. B. Robinson, and J. V. Waszczak, *ibid.* **64**, 2711 (1990).
³⁰U. Hartmann, T. Göddenhenrich, and G. Heiden, *J. Magn. Magn. Mater.* **101**, 263 (1991).
³¹Z. J. Yang, *Jpn. J. Appl. Phys.* **31**, L938 (1992).
³²P. G. de Gennes, *Superconductivity of Metals and Alloys* (Addison-Wesley, Reading, MA, 1989).
³³Q. P. Li, B. E. C. Koltenbah, and R. Joynt, *Phys. Rev. B* **48**, 437 (1993).
³⁴H. Won and K. Maki, *Phys. Rev. B* **49**, 1397 (1994).
³⁵G. Binnig, H. Rohrer, Ch. Gerber, and E. Weibel, *Phys. Rev. Lett.* **49**, 57 (1982).
³⁶R. Proksch and E. D. Dahlberg, *J. Appl. Phys.* **73**, 808 (1993).